A spot-forward model for electricity prices with regime shifts

Florentina Paraschiv[a,*], Stein-Erik Fleten[b], Michael Schürle[a]

[a] *Institute for Operations Research and Computational Finance, University of St. Gallen, Switzerland*
[b] *Department of Industrial Economics and Technology Management, Norwegian University of Science and Technology, Trondheim, Norway*

Abstract

We propose a novel regime-switching approach for electricity prices in which simulated and forecasted prices are consistent with currently observed forward prices. Additionally, the model is able to reproduce spikes and negative prices. We distinguish between a base regime as well as upper and lower spike regimes. We derive hourly price forward curves for EEX Phelix, and together with historical hourly spot prices, historical hourly price forward curves are the basis for model calibration. The model can be used for simulation and forecasting of electricity spot prices over short- and medium-term horizons. Tests imply that it shows a better performance than classical time series approaches.

Keywords: electricity prices, regime-switching model, negative prices, spikes, price forward curves

1. Introduction

The deregulation of electricity markets has shifted much risk onto producers and retailers. Extreme price movements force producers and wholesale buyers to hedge against price risk. Electricity is non-storable and faces a volatile demand from end-users depending on weather conditions and business cycles. Furthermore, factors like the use of renewable energy sources, power plant outages or transmission grid unreliability enhance complexity

*Corresponding author
Email address: florentina.paraschiv@unisg.ch (Florentina Paraschiv)

and reduce price predictability. Finding realistic models to describe electricity prices is essential for the valuation of power contracts, for risk managers for the estimation of risk measures as well as for portfolio managers for the identification of worst-case scenarios in very turbulent markets.

Dependent on the research question and planning task different models for electricity prices are proposed in the literature. Fundamental models take into account the components of the whole electricity system and serve for long-term planning (see [14]). Game theoretic approaches analyse the strategic behavior of different market participants ([11, 17]) and account for market design options. Financial mathematical models deal with the volatility of electricity prices and are often used for the evaluation of energy derivatives ([22]). Econometric time-series models like ARMA and GARCH processes are applied to simulate and forecast electricity prices for a short-term planning period and reflect specific patterns such as autocorrelation (see [7, 18, 27]).

The models discussed earlier describe in general typical characteristics of electricity prices like seasonality patterns, mean reversion or volatility clustering. However, beside these aspects, an important characteristic to be considered is the extreme price changes that are reflected by the so-called "spiking" behavior of power prices. These spikes occur mainly because electricity is non-storable which causes demand and supply to be balanced on a "knife-edge" (see [25]). Relatively small changes in the load or generation can cause extreme price changes between consecutive hours. The spiking behavior is often described in the literature by regime-switching models ([2, 12, 13, 25, 26, 27]). The authors conclude in general that regime switching models lead to a better modeling performance than the other models mentioned before. They additionally allow electricity prices to switch between a "base" regime and a "jump" regime. Jumps are modeled by a jump diffusion process, or the regimes are governed by an unobservable, stochastic process (Markov regime-switching models).

We propose a novel regime-switching approach for electricity prices in which simulated and forecasted spot prices are consistent with currently observed forward prices. Every day, futures prices are observed in the market and an hourly price forward curve (HPFC) is derived. The typical seasonality pattern of electricity prices is additionally used to model the curve. The forward price of a particular day and hour provides information on the expected spot price of that day/hour. This is used to generate simulations or forecasts of future spot prices. Since the HPFC extends to the longest available maturity of the instruments considered in its derivation, the price simulations or forecasts can range over longer time horizons with hourly resolution.

Our model distinguishes further between a base and two spike regimes and allows for spike clustering and for negative prices. This is important since prices jump into another spike regime and can remain there for some hours (see the discussion in [12] or [13]). Furthermore, negative prices occur at EEX since 1 September 2008 due to the special characteristics of electricity markets, e.g., limited storage capacities, limited load change flexibility and combined production of heat and power.

Most spot price simulation models cited earlier lack consistency with the market because the information about the expected future spot prices reflected in the forward curve is not taken into account. For risk management applications in particular, such as hedging of price risk or valuation of power contracts, consistency with the observed forward prices is essential. This means that forecasted and simulated spot prices are adjusted for risk, allowing for straightforward valuation procedures. Compared to classical time-series models, our regime-switching model also leads to a significantly better in- and out-of-sample fit and can be used for long-term simulations of spot prices with the current HPFC as input.

The idea of using information from the HPFC in a regime-switching model was also used in [16] in the context of scenario generation within a stochastic optimization model for medium-term power production planning. However, there deviations from the forward curve and spikes were modeled as independent events. We extend this approach by introducing also serial dependencies and a transition probability matrix to model spike clusters. Additionally, the variation of spot prices and spikes may now be season-dependent. For the generation of the input HPFC we use here a more suitable methodology to reflect the intra-day seasonality pattern.

This paper is organized as follows: In Section 2 we summarize characteristics of electricity spot prices and consequences for the model structure. Based on these considerations, Section 3 outlines the derivation of HPFCs and introduces the formal specification of the regime switching model. The corresponding estimation procedure is described in Section 4 and the obtained results are discussed in Section 5. In Section 6 we show the comparative performance of the regime-switching model versus classical time-series models and results of simulation runs. Section 7 discusses the use of the model for short- and medium-term forecasts. Finally, Section 8 concludes.

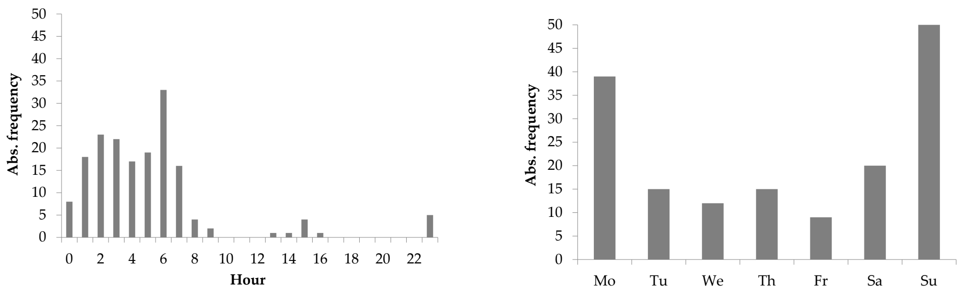

Figure 1: Occurrence of negative prices at EEX.

2. Characteristics of electricity prices and modeling assumptions

2.1. Preliminaries

Electricity prices have properties that differ considerably from those of other financial assets or even of other commodities (see [4, 13]). The yearly, weekly, and daily seasonal behavior of the electricity prices is one of the most complicated ones among commodities. This is due to the inelastic short-term demand for electricity, caused by economic and business activities. Combined with the lack of efficient storage opportunities, which prevents intertemporal smoothing of the demand, extremely large price movements (spikes) as well as various cyclical patterns of behavior occur. Besides, it is expensive or even damaging to change the production of big generating units abruptly, which are further causes for spikes and even negative electricity prices.

From an economic perspective, negative prices can be rational, e.g., if the costs of shutting down and ramping up a power plant unit exceed the loss for accepting negative prices (see [13]). Since 1 September 2008, negative price bids are allowed at the German power exchange EEX. Historical spot market data over the period from 1 September 2008 to 14 March 2013 show a total amount of about 174 hours with negative prices. As shown in Figure 1, negative prices occur mostly during the night and early morning hours (11 pm to 8 am). The distribution of negative prices over the week has a maximum on Sundays (including public holidays), the remaining observations are concentrated on Mondays.

2.2. Model architecture

2.2.1. Market view and seasonality

The prices on the futures market provide valuable information about the expected evolution of electricity prices. However, futures are only traded for

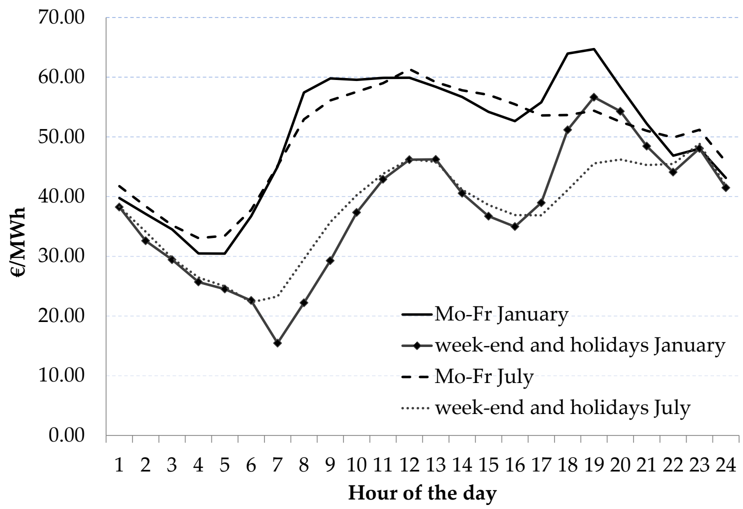

Figure 2: Hourly and daily day-ahead price patterns for EEX Phelix.

standard periods, e.g., for delivery over one month, quarter or year. Information about expected prices for individual hours must therefore be derived from the prices of traded instruments using the historically observed seasonal patterns. We can distinguish between yearly, weekly, and intra-day seasonality: The average price levels differ between summer and winter as well as between weekdays and weekend days. The load as a main driver for electricity prices shows a noticeable peak at midday during the summer months, or two peaks around noon and early evening in winter. As a consequence, prices at these hours are higher than, for example, during the night when demand is low (see Figure 2). Hence, we estimate a seasonality shape from historical spot prices that incorporates these aspects. From this we derive a HPFC in such a way that the hourly prices reflect the seasonal pattern and are consistent with the last observed prices of the traded instruments (see Appendix A for details). In this way, the current market view on the future spot price evolution is taken into account in our modeling approach.

To obtain forecast or simulations of future spot prices, we exploit the information contained in the HPFC, together with the day-ahead prices that are revealed every day at EEX around 2 pm. As shown in Figure 3, the day-ahead prices published in day 0 for day 1, together with the last generated HPFC that starts at midnight in day 2, can be used to forecast the spot prices for day 2. The spot prices are the result of the day-ahead auction in day 1 and, thus, such a prediction is meaningful up to the price publication

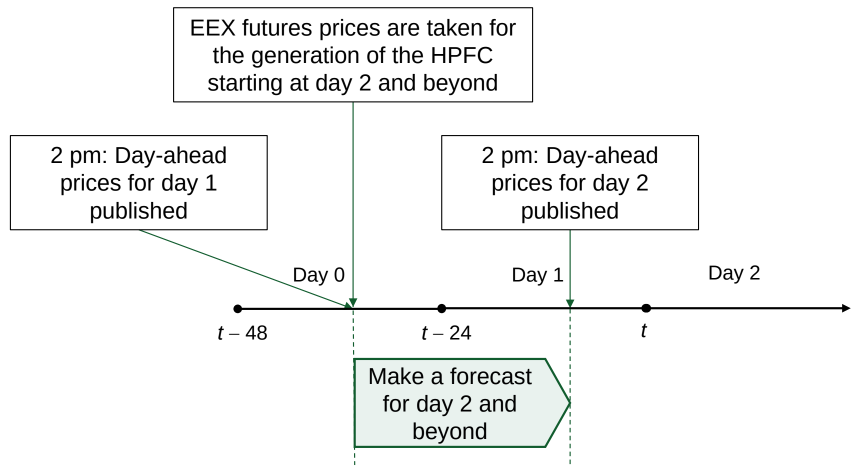

Figure 3: Availability of price information at EEX.

at 2 pm. In principle, this forecast can be extended beyond day 2 since the HPFC provides also forward prices for the subsequent period.

2.2.2. Stochastic component with three regimes

Besides the deterministic impact factors, electricity spot prices are also influenced by uncertainties like power plant outages and fluctuant renewable electricity generation. These uncertain factors are drivers of the stochastic component of the spot prices. An important characteristic of electricity prices is their spiking behavior: Prices may jump to an extremely high or low price level, stay there for some hours, and afterwards they jump back again to the original price level. Therefore, the stochastic fluctuation around the hourly price forward curve is described by a regime switching model where a base regime is distinguished from two spike regimes that reflect large price movements down- or upwards. A price is considered to be in one of the spike regimes if it is below or above some limit values which will be estimated simultaneously with the other model parameters. This allows for a more realistic fit to the data than the common approach in the literature where regime limits are set to three standard deviations (see [13]).

In the *base regime*, differences between spot and forward prices result from (not anticipated) deviations between the realized supply of and demand for electricity. Since the causes for this, e.g., weather conditions or power plant outages, may persist for some hours, prices of consecutive hours are in general highly correlated. Therefore, the differences in the logarithms of spot and forward prices are modeled by an autoregressive process. In comparison with

[12] or [13], who introduce also regime-switching models where prices in a base regime are driven by mean-reverting processes (e.g., Ornstein-Uhlenbeck), the choice of an autoregressive process with several lags is more flexible to reproduce the "spillover effects" of a change in the price level in a specific hour to the prices of subsequent hours. This is important since the electricity prices can change significantly over time.

On the other hand, in the two *spike regimes* deviations from the lower and upper limits that separate them from the base regime are by assumption exponentially distributed. In particular, this allows to model negative prices. The extreme price levels of spikes are seen as "isolated" events and do not carry over to later observations in the base regime. Therefore, we model them as independent events and, in particular, not dependent on exogenous variables like supply from renewable energies that are difficult to forecast.

2.2.3. Seasonal characteristics of price volatility and spikes

It can be observed empirically that electricity prices show different volatilities and jump behavior in different seasons (summer/winter), different days of the week (weekdays/weekend) and hours of the day (see [12, 13]). Therefore, the regime-switching model estimates different parameter sets for days in summer (1 April to 30 September) than in winter (1 October to 31 March). Likewise, parameters may differ for distinct times of the day as price volatility increases around noon in summer or in the early evening in winter.

2.2.4. Transition matrixes

A transition matrix is used to describe the probabilities of transitions between the three regimes. In this way, a "clustering" of extreme prices may be taken into account, i.e., a spike occurs with higher probability if already one was observed in the hour before. The importance of modeling spike clusters with transition matrixes is discussed, e.g., in [2, 12, 13]. For the derivation of transition matrix we distinguish also between seasons, days of the week, and times of the day. A similar approach can be found in [13], where transition probabilities between regimes are separately obtained for summer and winter.

3. Model specification

3.1. Derivation of the HPFC

We derive hourly price forward curves (HPFC) by application of the methodology described in [3], extended to hourly steps. The derived curves will serve as input for the spot-forward model. In the sequel we drop the times of the observations in the notation for simplicity. Let f_t be the price of the forward contract with delivery at time t, where time is measured in hours. The constructed hourly price forward curve f_t replicates the currently observed market prices $F(T^S, T^E)$ perfectly, where T^S and T^E are the start and end dates for different settlement periods:

$$F(T^S, T^E) = \frac{1}{T^E - T^S} \int_{T^S}^{T^E} f_t \, dt, \tag{1}$$

This considers the case that contracts are settled in T^E only. It is assumed that the HPFC can be decomposed into a seasonal component s_t and a residual or correction term ε_t. The seasonality shape is derived here following the approach in [4] (see Appendix A). The correction term is modeled by a polynomial spline function of the form

$$\varepsilon_t = \begin{cases} a_1 t^4 + b_1 t^3 + c_1 t^2 + d_1 t + e_1 & t \in [t_0, t_1) \\ a_2 t^4 + b_2 t^3 + c_2 t^2 + d_2 t + e_2 & t \in [t_1, t_2) \\ \vdots & \\ a_n t^4 + b_n t^3 + c_n t^2 + d_n t + e_n & t \in [t_{n-1}, t_n] \end{cases} \tag{2}$$

The curvature of this spline function is minimized according to a maximum smoothness criterion that was suggested in [1] for fitting interest rate curves. The "time knots" $\{t_0, t_1, ..., t_n\}$ are defined by the sorted start and end dates for the settlement periods of the futures that are taken into account. Additional constraints ensure the connectivity and smoothness at the knots (see [3] for details). The advantage of this approach is that the smoothness is calculated on the adjustment function ε_t and not on the forward function f_t in order to retain the seasonality pattern better. This is relevant for our application since the resulting price forward curves (PFCs) should incorporate the hourly pattern as well. Other approaches for the derivation of PFCs like [9] are less useful for that purpose because the "smoothing factor" introduced there eliminates the hourly seasonality pattern. This discussion can be followed in [3] and in [4].

3.2. Specification of the regime-switching model

As mentioned above, different parameters may be applied for distinct times of the day, days of the week, and seasons. Several successive hours with similar price characteristics are combined to blocks. Let H be the number of different parameter sets in the base regime for distinct hourly blocks dependent on the day of the week and the season. Then a function $h(t): \ t \rightarrow \{1, \ldots, H\}$ is defined which assigns to time t (measured in hours) the index h of the corresponding parameter set. For the spike regimes it is advisable to use a smaller number D of different parameter sets since there are considerably less observations of extreme prices available for the estimation. We will therefore distinguish only between days and seasons, and a function $d(t): \ t \rightarrow \{1, \ldots, D\}$ assigns to time t the corresponding day index d. In the sequel, the dependency of $h(t)$ and $d(t)$ on time will be dropped in the notation for simplicity.

Recall that differences between the logarithms of spot and forward prices are modeled by an autoregressive process in the base regime. The latter is separated by some limit values from the upper and the lower spike regime. The deviations of prices from these limits in the spike regimes are exponentially distributed. With the definitions

S_t	spot price in hour t
f_t	forward price in hour t derived from HPFC
r_t	deviation of spot price in t from HPFC in the base regime
ξ_t^+	upward spike, exponentially distributed with parameter λ_d^+
ξ_t^-	downward spike, exponentially distributed with parameter λ_d^-
f_t^U	upper limit of the base regime in hour t
f_t^L	lower limit of the base regime in hour t

the complete model for the spot price (or market clearing price) reads as follows:

$$S_t = \begin{cases} f_t^L - \xi_t^-, & \text{if the system is in the lower spike regime,} \\ f_t \cdot \exp(r_t), & \text{if the system is in the base regime or} \\ f_t^U + \xi_t^+, & \text{if the system is in the upper spike regime.} \end{cases} \tag{3}$$

The random variables in the three regimes are modeled by

$$\xi_t^- \sim \operatorname{Exp}(\lambda_d^-), \qquad \xi_t^+ \sim \operatorname{Exp}(\lambda_d^+) \tag{4}$$

for $d = 1, \ldots, D$, where $1/\lambda_d^-$ and $1/\lambda_d^+$ represent the expectations of the corresponding variables, and

$$r_t = a_h + \sum_{i \in \mathcal{L}} b_{i,h} \cdot \hat{r}_{t-i} + \varepsilon_t, \qquad \varepsilon_t \sim \mathrm{N}(0, \sigma_h^2) \tag{5}$$

for $h = 1, \ldots, H$ where $\mathcal{L}$ is a set of lag indices and

$$\hat{r}_{t-i} = \begin{cases} \ln S_{t-i} - \ln f_{t-i} & \text{if system is in base regime at time } t-i, \\ \mathrm{E}(r_{t-i}) & \text{otherwise.} \end{cases} \tag{6}$$

The last equation (6) implies that “missing” lagged observations of the base regime (which result if at time t a spike occurred) are replaced by their expectations. In this way, the extreme price levels of spike regimes have no impact on the prices in the base regime in subsequent hours.

For storable commodities, arbitrage-based arguments imply that forward prices are equal to (discounted) expected spot prices. Due to the non-storability of electricity, this link does not exist here. Therefore, it can be expected that forward prices are formed as the sum of the expected spot price plus a risk premium that is paid by risk-averse market participants for the elimination of price risk. The risk premium may be positive or negative, depending on the average risk aversion in the market. It may vary in magnitude and sign throughout the day and between seasons (cf. [21]). In our context, the premium for each block $h = 1, \ldots, H$ is related to the long-term mean of the autoregressive process (5), given that it is stationary:

$$\mu_h = \frac{a_h}{1 - \sum_{i \in \mathcal{L}} b_{i,h}} \tag{7}$$

The probabilities of remaining in the current regime or switching to another one from hour t to hour $t+1$ are modeled by a transition matrix Π_h, $h = 1, \ldots, H$, that has the structure

$$\Pi_h = \begin{pmatrix} 1 - \pi_h^{LB} & \pi_h^{LB} & 0 \\ \pi_h^{BL} & 1 - \pi_h^{BL} - \pi_h^{BU} & \pi_h^{BU} \\ 0 & \pi_h^{UB} & 1 - \pi_h^{UB} \end{pmatrix}. \tag{8}$$

For example, π_h^{BU} (π_h^{BL}) denotes the probability that in the next hour an upward (downward) spike occurs, given that the system is now in the base regime, and π_h^{UB} (π_h^{LB}) is the probability of a transition from the upper (lower) spike back to the base regime. As implied by the zeros, it is impossible that a downward spike is directly followed by an upward spike or vice versa, which also cannot be observed in historical data. Individual matrices for each time block take into account the different probabilities for the occurrence of spikes at day and night hours, as well as a distinction between weekdays and weekend days or seasons.

It remains to define when a price level is considered "extreme", i.e., the concrete values of the limits f_t^L and f_t^U that separate the base regime from the lower and the upper spike regime. They are derived from the forward prices f_t given in terms of the HPFC by

$$\begin{aligned} f_t^L &= f_t / \exp(\alpha_\delta^L) \\ f_t^U &= f_t \cdot \exp(\alpha_\delta^U), \end{aligned} \tag{9}$$

for the additional parameters $\alpha_\delta^L > 0$ and $\alpha_\delta^U > 0$. Again, the index δ allows a distinction between different days or seasons to take into account different spike characteristics.

4. Estimation procedure

4.1. Estimation of HPFCs

Following the procedure outlined in Section 3.1, we derive HPFCs based on the information about the market prices obtained each day between 1 January 2009 and 14 March 2013. An example for a smoothed forward curve is shown in Figure 4. It was generated for 3 January 2012 with market data from EEX Phelix observed on the day before. All in all, settlement prices of 30 weekly, monthly, quarterly, and yearly base contracts were used to construct a spline consisting of $n = 32$ polynomials. The HPFCs for the other days of the sample period are obtained analogously with updates of the market prices for each trading day. These curves represent the input for our spot model.

4.2. Estimation of model parameters

According to equation (9) the allocation of observations to the base, to the lower, or to the upper spike regime depends on the choice of the parameters α_δ^L and α_δ^U. Preliminary model tests implied that it is sufficient to distinguish between Sunday ($\delta := 2$) and the other days ($\delta := 1$). A further differentiation between seasons, other weekdays, or times of the day would not result in significantly different estimated values for α_δ^L and α_δ^U with our data set (results are available on request).

The remaining model parameters for the base and for the spike regimes depend now on the specific choice of α_δ^L and α_δ^U, $\delta \in \{1, 2\}$. The identification of the full parameter set consists therefore of two nested steps: In an "outer estimation" a log-likelihood function $\ln L(\alpha_1^L, \alpha_1^U, \alpha_2^L, \alpha_2^U)$, that will be

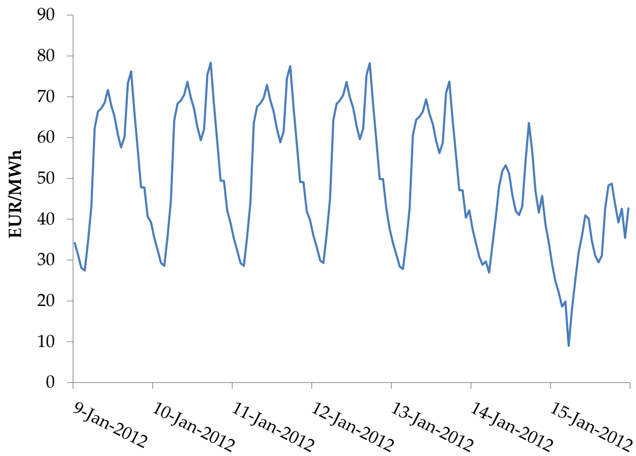

Figure 4: Hourly Price Forward Curve for EEX Phelix at 02/01/2012.

specified in the sequel, is maximized with respect to the parameters which separate the three regimes. In each step of this procedure observations are assigned to regimes based on the current values of α_δ^L and α_δ^U, $\delta \in \{1, 2\}$. Then the remaining model parameters are identified separately for each regime in an "inner estimation". We start with a description of the latter.

4.2.1. Estimation of expected spike magnitude and AR process parameters

Assume that the values of the parameters $\alpha_1^L, \alpha_1^U, \alpha_2^L, \alpha_2^U$ that define the limits of the base regime have been set in the "outer estimation" step. Based on this, the observations at (hourly) time points $t = 1, \ldots, T$ can be assigned to the different regimes. Define for each hourly time block $h' = 1, \ldots, H$ the sets

$$\mathcal{D}^B(h') := \{t = 1, \ldots, T \,|\, h(t) = h' \,\wedge\, f_t^L \leq S_t \leq f_t^U\}$$

of observations that belong to different time bands of the base regime and for each daily block $d' = 1, \ldots, D$ the sets

$$\mathcal{D}^L(d') := \{t = 1, \ldots, T \,|\, d(t) = d' \,\wedge\, S_t < f_t^L\}$$
$$\mathcal{D}^U(d') := \{t = 1, \ldots, T \,|\, d(t) = d' \,\wedge\, S_t > f_t^U\}$$

that contain the observations of the lower and upper spike regime. Note that the dependence of these sets – and likewise of the parameter estimates that result in this step – on the values of α_δ^L and α_δ^U, $\delta \in \{1, 2\}$, is dropped in the notation for simplicity. The parameter estimates for the exponential distributions of the spike magnitudes are given by the reciprocal values of the average deviations between spot prices and regime limits:

$$\hat{\lambda}_{d'}^{-} = \frac{\#\text{elements in } \mathcal{D}^L(d')}{\sum_{t \in \mathcal{D}^L(d')} (f_t^L - S_t)}, \qquad \hat{\lambda}_{d'}^{+} = \frac{\#\text{elements in } \mathcal{D}^U(d')}{\sum_{t \in \mathcal{D}^U(d')} (S_t - f_t^U)}.$$

To determine the parameters of the autoregressive process used to model the deviations $r_t := \ln S_t - \ln f_t$ in the base regime, the residuals e_t are calculated for all $t = 1, \ldots, T$:

$$e_t = \begin{cases} r_t - a_{h(t)} - \sum_{i \in \mathcal{L}} b_{i,h(t)} \cdot \hat{r}_{t-i}, & t \in \mathcal{D}^B(h(t)) \\ 0, & \text{otherwise} \end{cases} \tag{10}$$

Recall that a lagged value $\hat{r}_{t-i}$ equals the observation r_{t-i} unless a spike occurred at time $\tau := t - i$, then it is replaced by its expectation:

$$\hat{r}_\tau = \begin{cases} r_\tau, & \tau \in \mathcal{D}^B(h(\tau)) \\ a_{h(\tau)} + \sum_{j \in \mathcal{L}} b_{j,h(\tau)} \cdot \hat{r}_{\tau-j}, & \text{otherwise} \end{cases}$$

For all $h' = 1, \ldots, H$ the coefficients of the autoregressive processes introduced in equation (5) are estimated by minimizing the sum of the squared residuals defined in (10):

$$\min \sum_{t=1}^{T} e_t^2$$

Then, (unbiased) estimators for the volatility parameters of block $h' = 1, \ldots, H$ are obtained from the variances of the residuals defined in (5), calculated as the sum of the squared errors divided by sample size minus degree of freedom:

$$\hat{\sigma}_{h'}^2 = \frac{\sum_{t \in \mathcal{D}^B(h')} e_t^2}{\#\text{elements in } \mathcal{D}^B(h') - \#\text{elements in } \mathcal{L} - 1}$$

After the above listed parameters have been estimated, the value of the log-likelihood function

$$\ln L(\alpha_1^L, \alpha_2^L, \alpha_1^U, \alpha_2^U) = \sum_{h'=1}^{H} \sum_{t \in \mathcal{D}^B(h')} \ln \phi(e_t \,|\, 0, \hat{\sigma}_{h'}) + \sum_{d'=1}^{D} \sum_{t \in \mathcal{D}^L(d')} \ln \varphi(f_t^L - S_t \,|\, \hat{\lambda}_{d'}^-) + \sum_{d'=1}^{D} \sum_{t \in \mathcal{D}^U(d')} \ln \varphi(S_t - f_t^U \,|\, \hat{\lambda}_{d'}^+) \quad (11)$$

can be calculated for the given assignment of observations to regimes, where

$$\phi(x \,|\, \mu, \sigma) = \frac{1}{\sqrt{2\pi\sigma^2}}\, e^{-\frac{1}{2}\left(\frac{x-\mu}{\sigma}\right)^2}, \qquad \varphi(x \,|\, \lambda) = \begin{cases} \lambda e^{-\lambda x}, & x \geq 0 \\ 0, & x < 0 \end{cases}$$

are the densities of the normal and of the exponential distribution with parameters $\mu = 0, \sigma > 0$ and $\lambda > 0$, respectively.

4.2.2. Determination of limits between base and spike regimes

In the "outer estimation" step of the nested procedure we determine those values of $\alpha_1^L, \alpha_1^U, \alpha_2^L$ and α_2^U that allow for the best fit of the model to observations by maximization of the log-likelihood function (11). The downhill simplex method is used for this purpose (e.g., see [23, pp. 502–506]). After optimal values $\hat{\alpha}_1^L, \hat{\alpha}_1^U, \hat{\alpha}_2^L, \hat{\alpha}_2^U$ have been found, they are fixed and the log-likelihood function (11) is maximized once more with respect to the remaining model parameters to update the preliminary values found in the previously described "inner estimation". This provides consistent maximum likelihood estimates for the parameters of the three regimes, and their standard errors can be approximated from the outer products of the gradients of the log-likelihood function. The optimization itself is performed with the BFGS-algorithm from [23, pp. 521–526].

Finally, the elements of the transition matrix (8) are estimated from the absolute occurrences of transitions between regimes in successive hours. Define for $h' = 1, \ldots, H$ the sets of (transition) observations

$$\begin{aligned} \mathcal{D}^{BL}(h') &:= \{t = 1, \ldots, T-1 \,|\, h(t) = h' \,\wedge\, f_t^L \leq S_t \leq f_t^U \,\wedge\, S_{t+1} < f_{t+1}^L\} \\ \mathcal{D}^{BU}(h') &:= \{t = 1, \ldots, T-1 \,|\, h(t) = h' \,\wedge\, f_t^L \leq S_t \leq f_t^U \,\wedge\, S_{t+1} > f_{t+1}^U\} \\ \mathcal{D}_{-1}^{B}(h') &:= \{t = 1, \ldots, T-1 \,|\, h(t) = h' \,\wedge\, f_t^L \leq S_t \leq f_t^U\}. \end{aligned}$$

Then,

$$\hat{\pi}_{h'}^{BL} = \frac{\#\text{elements in } \mathcal{D}^{BL}(h')}{\#\text{elements in } \mathcal{D}_{-1}^{B}(h')}, \qquad \hat{\pi}_{h'}^{BU} = \frac{\#\text{elements in } \mathcal{D}^{BU}(h')}{\#\text{elements in } \mathcal{D}_{-1}^{B}(h')}$$

are the observed probabilities from moving from the base to the lower or upper spike regime for the hourly time band h', which takes into account that the probability of a spike occurrence may differ between day and night hours. For the estimation of the probabilities for transitions from a spike back to the base regime, we do not distinguish between different times of the day. This is again motivated by the fact that spikes, and in particular consecutive occurrences, are rare events and we expect to obtain more reliable results if the data are not split in too many subsamples. Therefore, we distinguish here only between D sets of transition probabilities analogously to the estimation of the expected spike magnitudes:

$$\begin{aligned}
\mathcal{D}^{LB}(d') &:= \{t = 1, \dots, T-1 \,|\, d(t) = d' \wedge S_t < f_t^L \wedge f_{t+1}^L \leq S_{t+1} \leq f_{t+1}^U\} \\
\mathcal{D}^{UB}(d') &:= \{t = 1, \dots, T-1 \,|\, d(t) = d' \wedge S_t > f_t^U \wedge f_{t+1}^L \leq S_{t+1} \leq f_{t+1}^U\} \\
\mathcal{D}_{-1}^{L}(d') &:= \{t = 1, \dots, T-1 \,|\, d(t) = d' \wedge S_t < f_t^L\} \\
\mathcal{D}_{-1}^{U}(d') &:= \{t = 1, \dots, T-1 \,|\, d(t) = d' \wedge S_t > f_t^U\}
\end{aligned}$$

for $d' = 1, \dots, D$. For the determination of the entries in the first and last row of the transition matrix defined in (8) for hourly blocks, we define a function

$$d^*(h(t)) : \; h(t) \to \{1, \dots, D\}$$

that assigns to the indices of the hourly time bands the corresponding day index. Then, the probabilities of moving from the lower or upper spike regime back to the base regime are estimated by

$$\hat{\pi}_{h'}^{LB} = \frac{\#\text{elements in } \mathcal{D}^{LB}(d^*(h'))}{\#\text{elements in } \mathcal{D}_{-1}^{L}(d^*(h'))}, \qquad \hat{\pi}_{h'}^{UB} = \frac{\#\text{elements in } \mathcal{D}^{UB}(d^*(h'))}{\#\text{elements in } \mathcal{D}_{-1}^{U}(d^*(h'))}.$$

5. Estimation results

We calibrate our model using as input HPFCs for each day between 1 January 2009 and 14 March 2013. From each single HPFC always the prices for the first day of each curve are extracted, i.e., the observations for the next 24 hours. This way we construct a "first-day HPFC" which contains updated information about the expected day-ahead prices for the next day. Focusing on the updated expectations is of great importance since electricity prices can change significantly also on short-term.

The regime-switching model is calibrated with the procedure described in the previous section. Recall that hours are combined to time blocks for

Table 1: Definition of blocks.

season	night	morning	high noon	afternoon	rush hour	evening
summer	1–6	7–10	11–14	15–18	–	19–24
winter	1–6	7–10	11–14	15–16	17–20	21–24

Table 2: Parameter estimates for the limits that separate the base from the lower and the upper spike regime for the three sample periods. Sunday has own parameters.

	01/01/2009–31/12/2010		01/01/2009–31/12/2011		01/01/2009–14/03/2013	
	Mo–Sa ($\delta = 1$)	Sun ($\delta = 2$)	Mo–Sa ($\delta = 1$)	Sun ($\delta = 2$)	Mo–Sa ($\delta = 1$)	Sun ($\delta = 2$)
$\hat{\alpha}^L_\delta$	0.50	0.99	0.50	0.85	0.69	0.91
$\hat{\alpha}^U_\delta$	0.78	1.15	0.78	1.11	0.80	1.05

which the same set of parameters are applicable. The definition of blocks that was used for our particular data set is shown in Table 1. This structure is motivated by the specification of some (non-overlapping) block contracts that are traded at the EEX/EPEX spot market and combine delivery over several hours (cf. [15, p. 45]).

For example, "night" covers the first six hours of the day (12:00 midnight to 5:59 a.m.), "morning" is the interval between the seventh and the tenth hour of the day (6:00 a.m. to 9:59 a.m.) etc. We define five blocks for summer while winter has one additional block to take into account the characteristic "evening peak" at this time of the year that becomes obvious in Figure 2. Furthermore, we distinguish between weekdays (Monday to Friday), Saturdays and Sundays, respectively, so that overall $H = 33$ different parameter sets must be estimated for the base regime. For the spike regimes we differentiate between the same days as before and between seasons, but not between hours. This leads to $D = 6$ different parameter sets for the distributions of spike magnitudes.

As motivated earlier, in case of the parameters for the limits that separate the base from the two spike regimes, it is not distinguished between seasons, different times of the day or weekdays, except that Sunday has its own parameters. The estimated values in Table 2 show a more extreme value for the latter since the price deviations in the base regime are more volatile here compared to the other days.

Tables 3 and 4 show the obtained transition probabilities for each hourly time block $h' = 1, \ldots, H$ and the expected magnitudes of downward and upward spikes $1/\hat{\lambda}^-_{d'}$ and $1/\hat{\lambda}^+_{d'}$, respectively, for the different days $d' = 1, \ldots, D$. We observe that, as expected, the probabilities for transitions from the base

Table 3: Estimation results for transition probabilities (in %). The upper part of the table shows the probabilities for transitions from the base to lower or upper spike regime for different hourly time bands. The lower part displays the probabilities for transitions from a spike regime back to the base regime, where no distinction is made between different times of the day. The meaning of the abbreviations is: S–Summer, W–Winter, Mo–Fr weekday, Sat–Saturday, Sun–Sunday.

			01/01/2009–31/12/2010		01/01/2009–31/12/2011		01/01/2009–14/03/2013	
seas.	day	hour	$\hat{\pi}_h^{BL}$	$\hat{\pi}_h^{BU}$	$\hat{\pi}_h^{BL}$	$\hat{\pi}_h^{BU}$	$\hat{\pi}_h^{BL}$	$\hat{\pi}_h^{BU}$
S	Mo–Fr	1–6	5.24	0.30	3.65	0.24	2.29	0.24
S	Mo–Fr	7–10	0.10	0.10	0.13	0.13	0.00	0.05
S	Mo–Fr	11–14	0.00	0.00	0.00	0.00	0.10	0.00
S	Mo–Fr	15–18	0.38	0.00	0.32	0.00	0.05	0.00
S	Mo–Fr	19–24	0.58	0.06	0.55	0.04	0.26	0.03
S	Sat	1–6	6.30	0.37	4.57	0.24	2.41	0.17
S	Sat	7–10	0.00	0.00	0.00	0.00	0.00	0.00
S	Sat	11–14	0.48	0.00	0.32	0.00	0.96	0.00
S	Sat	15–18	0.00	0.00	0.00	0.00	0.00	0.00
S	Sat	19–24	0.97	0.32	0.86	0.22	0.32	0.16
S	Sun	1–6	7.84	0.00	7.09	0.00	4.79	0.18
S	Sun	7–10	0.00	0.00	1.11	0.00	0.52	0.00
S	Sun	11–14	0.49	0.00	1.33	0.00	0.98	0.00
S	Sun	15–18	1.02	0.00	0.69	0.00	0.76	0.00
S	Sun	19–24	2.95	0.00	2.61	0.00	1.61	0.00
W	Mo–Fr	1–6	2.44	0.29	2.12	0.24	1.63	0.21
W	Mo–Fr	7–10	0.60	0.00	0.46	0.00	0.10	0.05
W	Mo–Fr	11–14	0.49	0.00	0.32	0.00	0.10	0.00
W	Mo–Fr	15–16	0.39	0.00	0.26	0.13	0.10	0.10
W	Mo–Fr	17–20	0.78	0.29	0.58	0.19	0.44	0.19
W	Mo–Fr	21–24	0.40	0.50	0.59	0.33	0.64	0.25
W	Sat	1–6	4.32	0.72	4.52	0.71	2.91	0.68
W	Sat	7–10	0.00	0.00	0.00	0.00	0.00	0.00
W	Sat	11–14	0.48	0.00	0.33	0.00	0.49	0.00
W	Sat	15–16	0.00	0.00	0.00	0.65	0.00	0.00
W	Sat	17–20	0.00	0.00	0.00	0.00	0.00	0.00
W	Sat	21–24	0.98	0.00	0.64	0.00	0.72	0.00
W	Sun	1–6	6.09	0.36	3.97	0.23	3.88	0.35
W	Sun	7–10	0.00	0.00	0.35	0.00	0.00	0.00
W	Sun	11–14	0.00	0.00	0.32	0.00	0.00	0.00
W	Sun	15–16	1.96	0.00	1.32	0.00	1.48	0.00
W	Sun	17–20	0.00	0.00	0.00	0.00	0.00	0.00
W	Sun	21–24	2.88	0.00	3.22	0.00	2.43	0.24
seas.	day	hour	$\hat{\pi}_h^{LB}$	$\hat{\pi}_h^{UB}$	$\hat{\pi}_h^{LB}$	$\hat{\pi}_h^{UB}$	$\hat{\pi}_h^{LB}$	$\hat{\pi}_h^{UB}$
S	Mo-Fr	–	65.40	53.85	66.77	46.67	65.74	55.00
S	Sat	–	60.78	87.50	64.52	87.50	64.81	87.50
S	Sun	–	70.24	95.83	69.92	95.83	68.33	92.00
W	Mo-Fr	–	65.22	80.36	65.29	77.78	69.86	76.32
W	Sat	–	73.08	33.33	75.00	33.33	71.43	85.71
W	Sun	–	65.00	0.00	68.92	0.00	71.00	77.78

Table 4: Estimation results for the expected downward and upward spike sizes $1/\lambda_d^-$ and $1/\lambda_d^+$ of the two spike regimes for different days and seasons. No distinction is made between hours of the day. Based on the calculation of standard errors, all model parameters are significant at 5% confidence level.

		01/01/2009–31/12/2010		01/01/2009–31/12/2011		01/01/2009–14/03/2013	
seas.	day	$1/\hat{\lambda}_d^-$	$1/\hat{\lambda}_d^+$	$1/\hat{\lambda}_d^-$	$1/\hat{\lambda}_d^+$	$1/\hat{\lambda}_d^-$	$1/\hat{\lambda}_d^+$
S	Mo-Fr	9.97	4.96	9.44	4.47	9.28	5.41
S	Sat	6.51	5.53	6.16	5.54	4.79	4.85
S	Sun	5.11	15.98	5.10	16.24	5.22	16.53
W	Mo-Fr	9.09	18.80	8.52	18.00	20.42	30.33
W	Sat	31.59	2.29	21.30	1.96	25.58	10.14
W	Sun	9.97	4.96	9.44	4.47	9.28	5.41

to the lower spike regime are slightly higher in summer, especially for the night hours and on Sundays. This is consistent with the observed occurrence of negative prices in the historical data. In summer the probabilities of upward spikes are smaller than for downward spikes, in particular on the weekend and in the night hours. There is a higher probability of upward spikes for working days in winter than in summer. This is due to the higher demand in winter than in summer time which makes prices more volatile.

The lower part of Table 3 shows the probabilities of transitions from a spike regime back to the base regime. The differences of these numbers to 100% correspond to the probabilities of remaining in the current spike regime. These values are considerably large compared to the probabilities of the spike regimes, given the system is currently in the base regime, which are displayed in the upper part of the table. This result reflects the "clustering" of extreme prices that is observable in the data. Furthermore, the expected spike magnitudes tend to be significantly larger in winter than in summer as the comparison in Table 4 implies, in particular for the last sample period.

For the estimation of the autoregressive process in the base regime we tested lags up to 24. A general observation is that coefficients of lags larger than six are not significant, except for the lag 24. This implies that spillover effects of not-anticipated events usually vanish after some hours, but some events may affect the price of the same hour on the next day. Thus we set $\mathcal{L} = \{1, \ldots, 6, 24\}$ for the subsequent analyses. Because of space restrictions not all estimates for the $H = 33$ parameter sets can be shown here. Figure 5 displays the long-term means of the autoregressive processes defined in (7) that result from the estimated parameters for the different time blocks and sample periods, separated for summer and winter. Overall, the deviations between spot and forward prices are close to zero for weekdays (Mo–Fr) and increase in absolute value on the weekend. In general, the magnitudes and signs vary between the blocks but are also different for the sample periods under consideration. This implies that the means of the modeled deviations are not constant over time.

The actual risk premium, which is defined as difference between forward minus spot price expectation, was derived from 1000 scenarios simulated with our regime-switching model and is displayed in Figure 6. The magnitudes are higher in winter than in summer, and premiums are positive during the week and decrease or become negative for the weekend. Also here a variation over time can be seen, which is consistent with the observed risk premiums in [20].

6. Simulation

As a test for model robustness we performed in- and out-of-sample simulation analyses where we evaluated the performance of the regime-switching approach versus the two time-series models: Autoregressive Moving Average (ARMA) models and General Autoregressive Conditional Heteroscedasticity (GARCH) processes. ARMA and GARCH models are often applied to electricity price simulations. They describe typical patterns of the historical price curves like autocorrelation that are related to external impact factors like electrical load or temperature.

6.1. Time series models

The specification of the ARMA process reads:

$$X_t = c + \sum_{i=1}^{p} \alpha_i X_{t-i} + \sum_{j=1}^{q} \beta_j \varepsilon_{t-j} + \varepsilon_t. \tag{12}$$

The parameters α_i describe the impact of the values X_{t-i} on the current value X_t for all lags $i = 1, ..., p$. The parameters β_j define the weights of the error terms (innovations) ε_j within the moving average component. For an extensive discussion and applications of ARMA models for electricity prices see [13].

Typically ARMA models are used in time series analysis to account for linear serial dependence. They provide the possibility to condition the mean

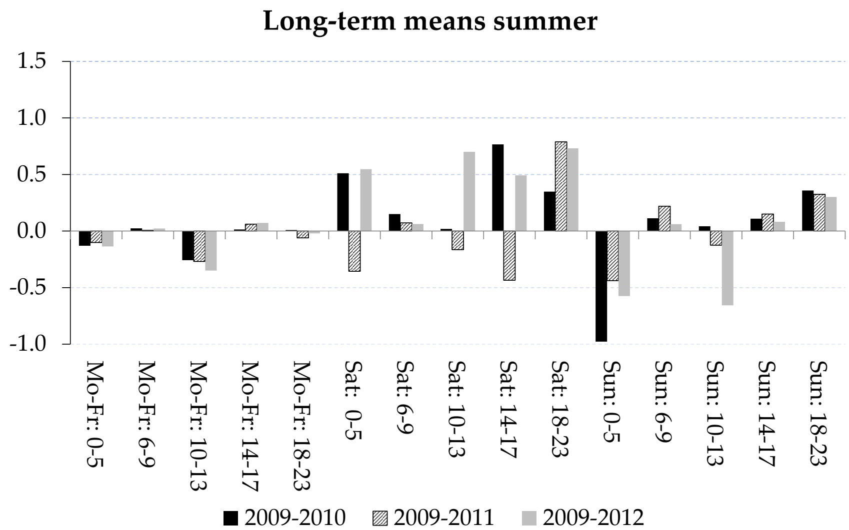

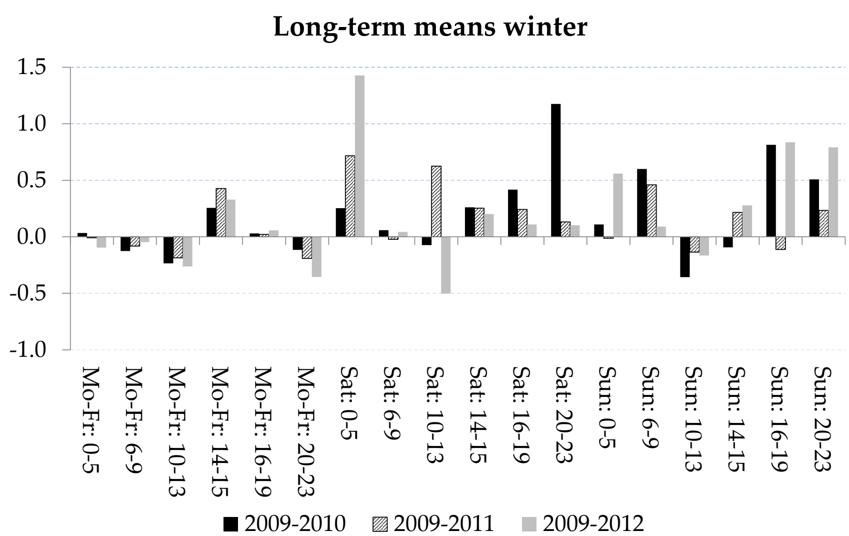

Figure 5: Long-term means of autoregressive process for the different blocks in summer (above) and winter (below).

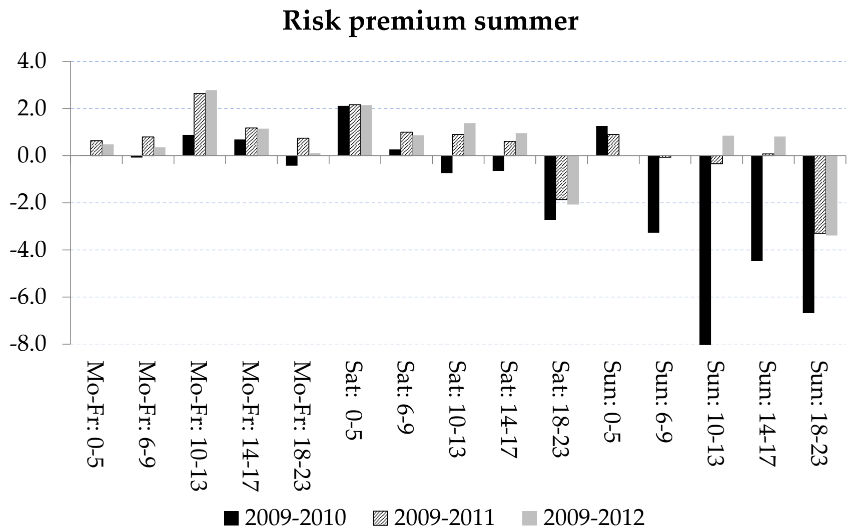

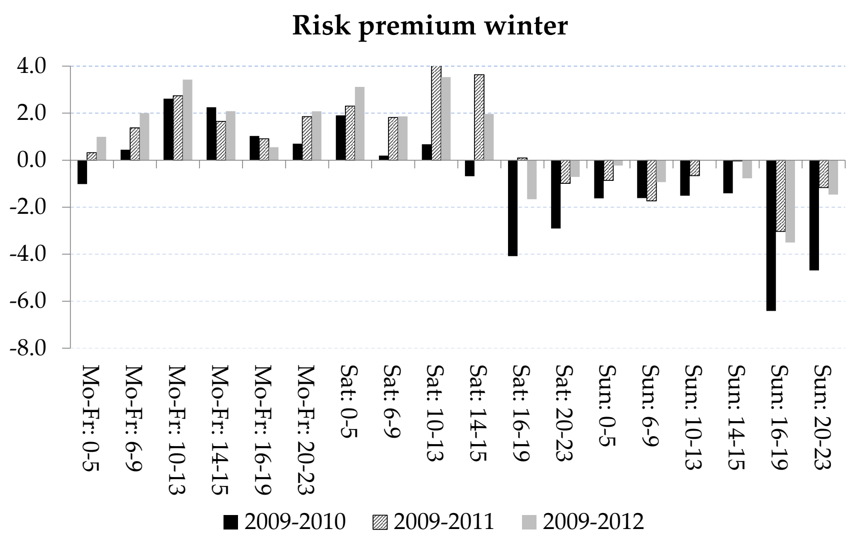

Figure 6: Risk premium derived from 1000 scenarios for summer (above) and winter (below).

Table 5: Engle's ARCH test: tested for the lags: 12, 24, 168 of the ACF. "H" is the vector of Boolean decisions for the tests. Values of H equal to 1 indicate rejection of the null of no ARCH effects in favor of the alternative.

H	p-value	statistics	critical value
1	0	1430.537	21.026
1	0	1457.811	36.415
1	0	1492.965	199.244

of the process on past realizations which has often produced acceptably accurate predictions of time series in the short term. However, the assumption of the autoregressive model of conditional homoscedasticity is too constricting, as electricity prices usually display volatility clusters or spikes (see [13]).

Within the GARCH approach the assumption of homoscedasticity is dropped in favor of a heteroscedastic variance. The GARCH(p, q) process according to [5] and [8] reads:

$$\sigma_t^2 = \phi_0 + \sum_{z=1}^{m} \phi_{1z}\sigma_{t-z}^2 + \sum_{y=1}^{n} \phi_{2y}\varepsilon_{t-y}^2 \tag{13}$$

The time-variant variance σ_t^2 is driven by a constant component ϕ_0, an autoregressive part of order m and a moving average part of order n. The variance at any time t must be positive and in consequence the parameters ϕ_0, ϕ_{1z} and ϕ_{2y} can take only nonnegative values at any time. We tested for ARCH and GARCH effects in the stochastic component of electricity prices employing Engle's ARCH test. The test results displayed in Table 5 show significant evidence in support of ARCH and GARCH effects.

We estimate ARMA(1,1), ARMA(5,1) and GARCH(1,1) models for the stochastic component of electricity prices. To this end, we first deseasonalize the electricity prices following the procedure applied in Appendix A and model their stochastic component. The model order is identified by looking at the Akaike's Information Criteria. Similar model orders were tested for electricity prices by [13]. We determine the model parameters by maximum likelihood estimation. The stability of the model parameters has been checked by estimating the parameters of different model versions for several sample periods separately: 01/01/2009–31/12/2010, 01/01/2009–31/12/2011 and 01/01/2009–14/03/2013. Table 6 summarizes the estimation results. We observe that model parameters are not sample dependent with exception of the ARMA(5,1) model, where the stability is less conclusive.

Table 6: Estimation results.

Sample		ARMA(1,1)	ARMA(5,1)	GARCH(1,1)
01/01/2009–	c	0.035	0.035	
31/12/2010	α_i	0.825*	0.763*, 0.051, -0.018, 0.009*, 0.020*	
	β_j	0.168*	0.228	
	ϕ_0			-’2.167*
	ϕ_{1z}			0.046*
	ϕ_{2y}			0.900*
01/01/2009–	c	-0.08	-0.005	
31/12/2011	α_i	0.827*	1.765*, -0.903*, 0.161*, -0.062*, 0.028*	
	β_j	0.079*	-’0.877*	
	ϕ_0			-’2.135*
	ϕ_{1z}			0.015*
	ϕ_{2y}			0.948*
01/01/2009–	c	0.058*	0.086*	
14/03/2013	α_i	0.879*	0.409*, 0.394*, 0.026*, 0.021*, -0.031*	
	β_j	0.0003	0.470*	
	ϕ_0			1.657*
	ϕ_{1z}			0.016*
	ϕ_{2y}			0.892*

6.2. In- and out-of-sample simulation results

After calibrating the models, several simulations were carried out to evaluate the goodness-of-fit of each stochastic model for electricity price simulation. In the case of the ARMA/GARCH models we first simulate the stochastic component of electricity prices, then we add the seasonality shape to get finally spot prices. With the novel regime-switching approach we directly simulate the electricity prices since the seasonality shape is incorporated already in the input HPFC. 1000 simulations are carried out over the three different sample periods. To show the in-sample model performance we assess the mean average percentage error ($MAPE$) over 1000 scenarios as well as the R^2. The $MAPE$ represents the normalized deviation of simulated prices from historical ones in absolute numbers:

$$\mathrm{E}(MAPE) = \frac{1}{N}\sum_{k=1}^{N}\frac{1}{T}\sum_{t=1}^{T}\frac{\left|S_{k,t}^{sim} - S_t\right|}{S_t} \tag{14}$$

where N is the number of simulated scenarios T is the time horizon and $S_{k,t}^{sim}$ is the simulated price in path $k = 1,\ldots,N$ at time $t = 1,\ldots,T$. The $MAPE$ is calculated for the sorted simulated price paths and the sorted real prices, also called price duration curves (PDC) (see [13, p. 12])

In Figure 7 we show a graphical comparison of in-sample simulated and historical prices for an arbitrary week (first week of March 2009). It can be

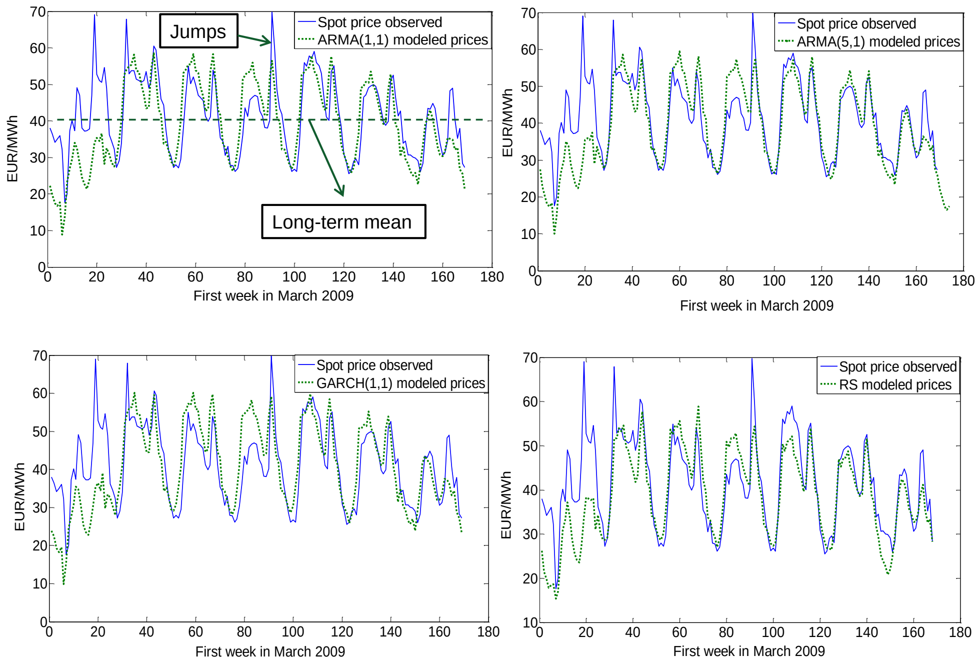

Figure 7: Historical and simulated price curves of different price models for a week.

Table 7: Expected $MAPE$ and R^2 for different stochastic models and different samples based on 1000 in-sample simulations.

Sample		ARMA(1,1)	ARMA(5,1)	GARCH(1,1)	RS model
01/01/2009–31/12/2010	$MAPE$	0.135	0.136	0.095	**0.079**
	R^2	0.490	0.493	0.490	**0.607**
01/01/2009–31/12/2011	$MAPE$	0.144	0.143	0.096	**0.084**
	R^2	0.442	0.442	0.439	**0.652**
01/01/2009–14/03/2013	$MAPE$	0.150	0.15	0.086	**0.083**
	R^2	0.414	0.414	0.409	**0.617**

seen that the simulated electricity price curves of all price models are similar to the observed price curves. Simulated electricity prices possess also daily, weekly, and annual cycles, which is caused by the deterministic shape component. Other important properties such as single peak, jump groups, or mean-reversion are also generated within the simulated price paths. Statistics about the in-sample performance of the various models over different investigated sample periods can be found in Table 7. The R^2 of our regime-switching model is 50% higher than for the other tested models while generally the $MAPE$ could be reduced.

For an assessment of the out-of-sample performance, we simulated 1000

Table 8: Expected $MAPE$ and R^2 for different stochastic models and different samples based on 1000 out-of-sample simulations.

Sample		ARMA(1,1)		ARMA(5,1)		GARCH(1,1)		RS model
		shape	HPFC	shape	HPFC	shape	HPFC	
01/01/2011–	$MAPE$	0.162	0.146	0.163	0.146	0.147	0.146	**0.088**
14/03/2013	R^2	0.119	0.155	0.112	0.156	0.123	0.167	**0.552**
01/01/2012–	$MAPE$	0.204	0.235	0.204	0.235	0.239	0.250	**0.095**
14/03/2013	R^2	0.110	0.109	0.104	0.102	0.112	0.100	**0.509**

scenarios starting at 01/01/2011 and 01/01/2012, respectively, for the time horizon up to 14/03/2013, when our data set ends. The parameters were estimated from the sample periods that ended just before the beginning of the simulations, i.e., no information on the stochastic dynamics was used from data observed after the start of the out-of-sample period.

In the previous in-sample simulation of the time series models the seasonality shape was aligned to the historic yearly average spot prices as described in Appendix A. For the out-of-sample test the historical price level must be replaced by some prediction of the future price level where we consider two approaches: Firstly, the (relative) seasonality shape is multiplied with the prices of base futures observed at the beginning of the simulation period to obtain the (absolute) seasonality component s_t. Secondly, we use the HPFC which is obtained after adding the correction term ϵ_t to s_t as outlined in Section 3.1. This allows us to decompose the out-of-sample performance of the time series models into the contributions of the pure deseasonalization (by the shape) and the additional correction included in the HPFC construction.

The results in Table 8 show that including the correction term improves the statistics (lower $MAPE$, higher R^2) only for the first period. In the second period the pure seasonality shape leads to better results, but in both cases the differences are small. An explanation is that the relevant information on the future spot price level plus seasonality pattern is already contained in the shape s_t (which is generally not consistent with all observed futures prices). The hourly forward prices f_t deviate from it to ensure consistency of the HPFC with all traded futures, where the deviation is "minimized" according to a smoothing criterion subject to constraints regarding the shape of the adjustment function ϵ_t. However, this correction can worsen the prediction as it does not add more information about the expected price level.

The regime-switching model shows again significantly better results than the benchmarks. It is by construction based on the HPFC for applications where consistency with the observed prices of traded standard products is relevant. From the comparison of the two types of deterministic components for the time series models (only deseasonalization vs. deseasonalization plus correction), we can conclude that the improvement is not due to the additional correction of the seasonality shape but fully explained by the regime-switching approach.

7. Forecasting

Our model may be used to forecast spot prices before the results of the day-ahead auctions are published (daily around 2 pm, see Figure 3). Additionally, we can generate long-term forecasts with hourly resolution for spot prices. Using the latest generated HPFC as input, the forecasting horizon can be extended to medium or long terms. We performed price forecasts for one week and one month for winter and summer. The benchmarks for the simulation studies (ARMA and GARCH) cannot be applied here because the predicted values converge quickly to the long-term mean and, thus, they are not appropriate for medium- or long-term forecasting. In fact, they are generally used in the literature (see [7, 19, 10]) for day-ahead forecasts of electricity prices.

Alternatively, ARMA models are justified if electricity prices are weak-stationary. However, the expected value of electricity prices and the variance might change over time, thus the assumption of weak-stationarity is too constricting (cf. [13]). The behavior of electricity prices in different periods is distinguished by slowly changing levels, or locally deviating trend slopes. It is therefore required to apply integrated ARMA (ARIMA) models that use linear filters to transform time series from not weak-stationary in weak-stationary ones. An additional advantage of this type of models is that they can be applied directly to the level of the prices (cf. [24]) or to log prices (cf. [6]). The seasonality of prices is taken into account by estimating a multiplicative ARIMA model. For an assessment which polynomial coefficients should be considered, we exploited the information of the autocorrelation and partial autocorrelation plots. The final model specification reads:

$$
\begin{aligned}
&(1-\phi_1 B^1-\phi_2 B^2-\phi_3 B^3-\phi_4 B^4-\phi_5 B^5-\phi_6 B^6)(1-\phi_{24} B^{24}-\phi_{48} B^{48}\\
&\quad -\phi_{72} B^{72}-\phi_{96} B^{96}-\phi_{120} B^{120}-\phi_{144} B^{144}-\phi_{168} B^{168})(1-B^1)\\
&\quad (1-B^{24}) S_t = c+(1-\theta_1 B^1-\theta_2 B^2-\theta_3 B^3-\theta_4 B^4-\theta_5 B^5-\theta_6 B^6)\\
&\quad (1-\theta_{24} B^{24}-\theta_{48} B^{48})(1-\theta_{168} B^{168})\varepsilon_t
\end{aligned}
$$

Table 9: *MAPE* and R^2 for forecasts of electricity spot prices over one week and one month in January and July with the regime-switching model in comparison with ARIMA.

Starting date		one week		one month	
		ARIMA	RS model	ARIMA	RS model
09/01/2012	*MAPE*	0.374	**0.133**	0.476	**0.134**
	R^2	0.01	**0.152**	0.01	**0.325**
02/07/2012	*MAPE*	0.125	**0.078**	0.099	**0.049**
	R^2	0.581	**0.792**	0.582	**0.659**

The ARIMA-generated hourly price forecast depends on previous values of prices as a product of 4 terms: 1 to 6 hours ago, one day ago to one week ago, hourly differentiation, and daily differentiation. It also depends on previous values of errors: 1 to 6 hours ago, 1 to 2 days ago and 1 week ago. A similar approach can be found in [6]. We fitted the model to the level of prices, since we aim at forecasting as well negative prices. For consistency, the sample period used in the estimation is the same as for the RS model. Tests have shown that for horizons longer than one month, ARIMA price forecasts deviate too much from the observed prices. For this reason, the model is also not appropriate for long-term in- or out-of-sample simulations. We therefore restrict ourselves to apply ARIMA for weekly and monthly price forecasts.

A comparison between the forecasting performance of the regime-switching model versus the ARIMA model is shown in Figures 8 and 9. We distinguish between a week (month) in summer and winter since the volatility of prices can have different patterns for these two seasons. For winter we compute price forecasts for January and for summer we forecasted the prices in July. Both models predict in a realistic way the typical intra-day seasonality of electricity prices. However, we observe that in January, when the level of the prices changes considerably among consecutive days, the ARIMA model significantly underestimates the realized price.

By contrast, the ARIMA model forecasts in a realistic way the prices for one week and one month in July, where there are no high price variations. These results are confirmed by the statistics in Table 9. The regime-switching model generates weekly and monthly forecasts with consistently smaller errors. *MAPEs* are larger for the price forecasts in winter, but still up to three times lower than in the case of ARIMA. Overall, the forecasts obtained by the regime-switching model are more robust among different samples. The regime-switching model is based on the identification of price regimes and transition matrices with a rigorous analysis of spike characteristics, and it

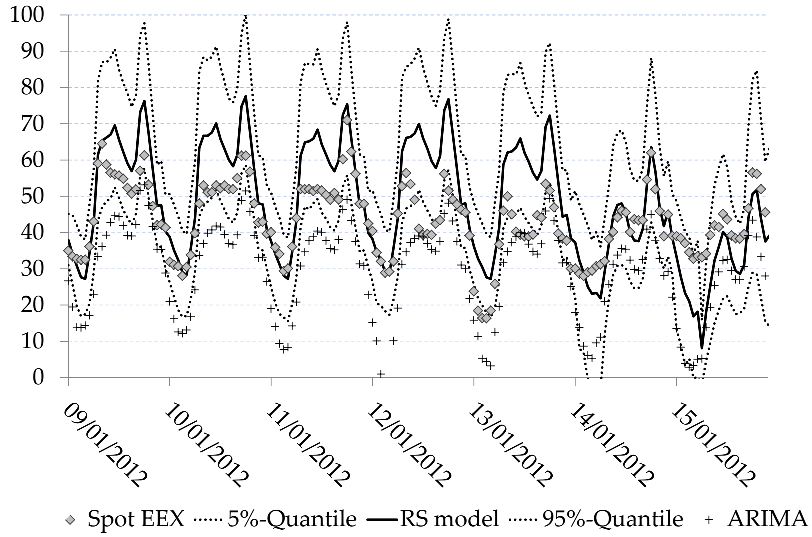

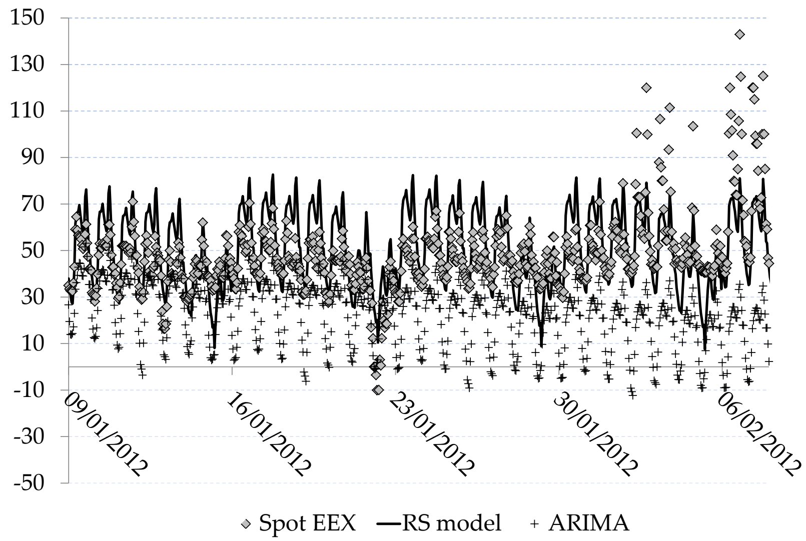

Figure 8: Spot price forecast for one week (above) and one month (below) starting on 09/01/2012. The quantiles in the upper graph refer to the limits of a 90%-prediction interval obtained from the RS model.

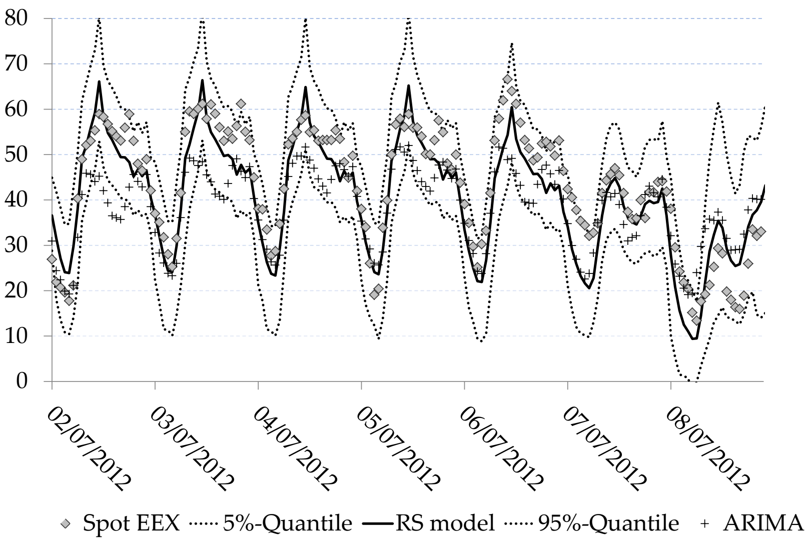

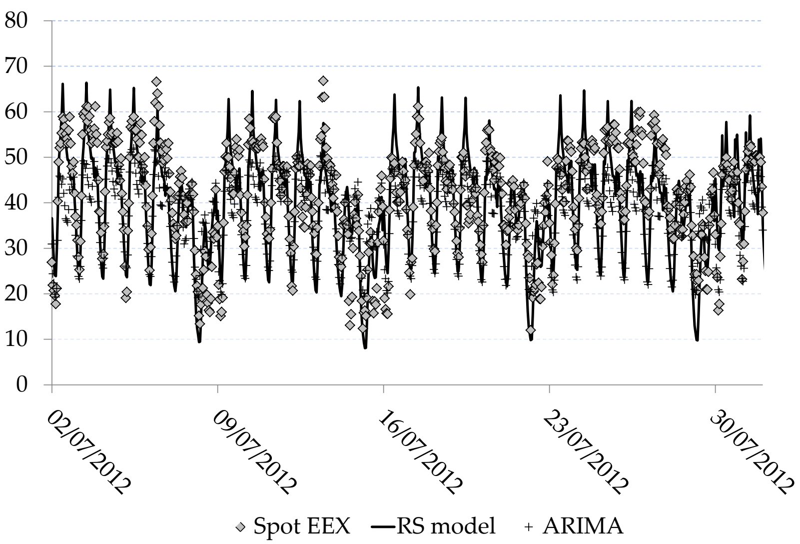

Figure 9: Spot price forecast for one week (above) and one month (below) starting on 02/07/2012 (see also Figure 8).

incorporates the market view. We therefore obtain better price forecasts than in the case of classical time series models.

8. Conclusions

In this paper, we proposed a new regime-switching approach for electricity prices. The expectation of the spot price is based on the market view reflected by price forward curves. Spot prices are allowed to vary around the hourly price forward curve (HPFC). The model distinguishes between a base and two spike regimes. Regime limits are estimated and not pre-defined. It is common in the literature to model the base regime by a mean-reversion process. Between successive hours high correlations can be observed. To take this into account we model the variations of spot prices around the HPFC in the base regime with an autoregressive process. Additionally, important characteristics of electricity prices like spike clusters and negative prices are reflected by the proposed regime-switching model.

We calibrated the model looking at different hourly blocks and we further differentiate between weekdays and weekends or between summer and winter seasons. This is important since it can be empirically observed that electricity prices show different volatilities and spike behavior dependent on the time of the day, weekday or season. The estimated probabilities confirm this observation. We found clear evidence for spikes clusters, which is consistent with the existing literature (see [12, 13, 25, 26, 27]).

The main advantage of the proposed spot-forward model is that it incorporates the market expectation contained in the HPFC with an hourly resolution, which is an important information for the building of spot prices. Classical time-series models use only historical data, but no information about the future. We showed that the regime-switching model leads to significantly better in- and out-of-sample results than classical time series models when it is applied for simulations and forecasts of spot prices over short- and medium-term horizons. In addition, the model can be used for long-term simulations of hourly spot prices based on the current HPFC. In this way, it may be integrated in applications like medium- and long-term planning for thermal electricity production and in general for the valuation of power contracts.

Appendix A. Derivation of the seasonality shape

In a first step, we identify the seasonal structure during a year with daily prices. In a second step, the patterns during a day are analyzed using hourly prices. Let us define two factors, the factor-to-year ($f2y$) and the factor-to-day ($f2d$). By $f2y$ we denote the relative weight of an average daily price compared to the annual base of the corresponding year:

$$f2y_d = \frac{S^{day}(d)}{\sum_{k \in \text{year}(d)} S^{day}(k) \frac{1}{K(d)}} \tag{A.1}$$

$S^{day}(d)$ is the daily spot price in the day d, i.e., the mean of the hourly electricity prices. $K(d)$ denotes the number of days in the year when $S^{day}(d)$ is observed. The denominator is thus the annual base of the year of the observation of $S^{day}(d)$. We estimate a regression model where the variation of the $f2y$ in the past is explained by dummy variables for the different months and historic temperature data.

The $f2d_t$, in contrast, represents the weight of the price of a particular hour compared to the daily base price

$$f2d_t = \frac{S^{hour}(t)}{\sum_{k \epsilon \text{day}(t)} S^{hour}(k) \frac{1}{24}}, \tag{A.2}$$

where $S^{hour}(t)$ is the spot price at the hour t. Again, we estimate a regression model for the $f2d$ with dummy variables for different day types (workdays are distinguished from weekend days and holidays) and seasons.

For the HPFC construction we obtain forecasts of the two factors defined in (A.1) and (A.2) from the estimated regression models and an additional model for the variation of the temperature over the year. Then, a (relative) seasonality shape sw_t can be calculated as $sw_t = f2y_t \cdot f2d_t$. In the last step, the forecasts for sw_t are multiplied with yearly average prices to align the shape to the price level. This yields the (absolute) seasonality shape s_t which is used for the derivation of the HPFC. It is updated each time when the HPFC is generated. For details on the regression models we refer to [4].

Figure A.10 shows the autocorrelation function of the hourly prices before and after deseasonalizing. Although there is still some seasonality left, results are acceptable, given the considerable initial autocorrelation between the values of same hours of different days and between the same days of different weeks.

[1] Adams, K.J., van Deventer, D.R., 1994. Fitting Yield Curves and Forward Rate Curves with Maximum Smoothness. Journal of Fixed Income **4**, 52–62.

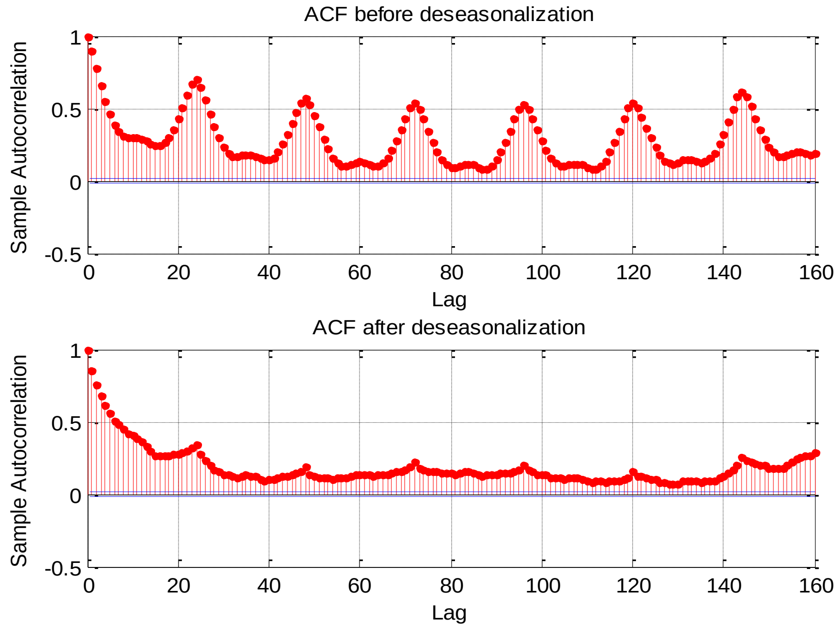

Figure A.10: Autocorrelation function before and after deseasonalization.

[2] Arvesen, Ø., Medbø, V., Fleten, S.-E., Tomasgard, A., Westgaard, S., 2013. Linepack storage valuation price uncertainty. Energy **52**, 155–164.

[3] Benth, F.E., Koekebakker, S., Ollmar, F., 2007. Extracting and applying smooth forward curves from average-based commodity contracts with seasonal variation. The Journal of Derivatives **15(1)**, 52–66.

[4] Blöchlinger, L., 2008. Power prices – a regime-switching spot/forward price model with Kim filter estimation, PhD thesis, University of St. Gallen.

[5] Bollerslev, T., 1986. Generalized autoregressive conditional heteroscedasticity. Journal of Econometrics **31(3)**, 307–327.

[6] Conejo, A.-J., Contreras, J., Espinola, R., Plazas, M.-A., 2005. Forecasting electricity prices for a day-ahead pool-based electric energy market, International Journal of Forecasting, **21**, 435–462.

[7] Contreras, J., Espinola, R., Nogales, F.J., Conejo, A.J., 2003. ARIMA

models to predict next-day electricity prices. IEEE Transactions on Power Systems, **18(3)**, 1014–1020.

[8] Engle, R.F., 1982. Autoregressive conditional heteroschedasticity with estimates of the variance of United Kingdom Inflation. Econometrica, **50(4)**, 987–1007.

[9] Fleten, S.-E., Lemming, J., 2003. Constructing forward price curves in electricity markets. Energy Economics **25**, 409–424.

[10] Garcia, R.C., Contreras, J., van Akkeren, M., Garcia, J.B.C., 2005. A GARCH forecasting model to predict day-ahead electricity prices. IEEE Transactions on Power Systems **20**, 867–874.

[11] Hobbs, B.F., 2001. Linear complementarity models of Nash-Cournot competition in bilateral and POOLCO power markets. IEEE Transactions on Power Systems **16(2)**, 194–202.

[12] Huisman, R., De Jong, C., 2003. Option pricing for power prices with spikes. Energy Power Risk Management **7(11)**, 12–16.

[13] Keles, D., Genoese, M., Möst , D., Fichtner, W., 2011. Comparison of extended mean-reversion and time series models for electricity spot price simulation considering negative prices. Energy Economics **34**, 1012–1032.

[14] Keles, D., Möst, D., Fichtner, W., 2011. The development of the German energy market until 2030 – A critical survey of selected scenarios. Energy Policy **39(2)**, 812-825.

[15] Konstantin, P., 2009. Praxisbuch Energiewirtschaft, 2nd ed. Springer.

[16] Kovacevic, R., Paraschiv, F., 2013. Medium-term planning for thermal electricity production. OR Spectrum, DOI:10.1007/s00291-013-0340-9.

[17] Lise, W., Linderhof, V., Kuik, O., Kemfert, C., Östling, R., Heinzow, T., 2006. A game theoretic model of the Northwestern European electricity market – market power and the environment. Energy Policy **34(15)**, 2123–2136.

[18] Misiorek, A., Trück, S., Weron, R., 2006. Point and interval forecasting of spot electricity prices: linear vs non-linear time series models. Studies in Non-linear Dynamics and Econometrics, **10(3)**, article 2.

[19] Nogales, F.J, Contreras, H., Conejo, A.J., Espinola, R., 2002. Forecasting day-ahead electricity prices by time-series models. IEEE Transactions on Power Systems **17**, 342–348.

[20] Paraschiv, F., Erni, D., Pietsch, R., 2014. The impact of renewable energies on EEX day-ahead electricity prices. Energy Policy, DOI:10.1016/j.enpol.2014.05.004.

[21] Pietz, M., 2009. Risk premia in electricity wholesale spot markets – empirical evidence from Germany. Working Paper, Center for Entrepreneurial and Financial Studies, Technical University of Munich.

[22] Weber, C., 2005. Uncertainty in the Electric Power Industry. Springer, New York.

[23] Press, W.T., Teukolsky, S.A., Vetterling, W.T., Flannery, B.P., 2007. Numerical Recipes: The Art of Scientific Computing, 3rd ed. Cambridge University Press.

[24] Syben, O. and T. Hatakka, 2013. Vergleich unterschiedlicher Ansätze für die Prognose von EEX-Spotpreisen. VDI-Berichte 2212, 133-141.

[25] Weron, R., Bierbrauer, M., Trück, S., 2004. Modeling electricity prices: jump diffusion and regime switching. Physica A **336**, 39–48.

[26] Weron, R., 2009. Heavy-tails and regime-switching in electricity prices. Mathematical Methods in Operations Research **69**, 457–473.

[27] Weron, R., Misiorek, A., 2005. Forecasting spot electricity prices with time series models. Proceedings of the European Electricity Market EEM-05 Conference, Lodz, 133–141.